CATHODIC SATURATION CURRENT OF THE HYDROGEN EVOLUTION REACTION ON NICKEL IN ALKALINE SOLUTIONS

By

Hideaki KITA and Tadayoshi YAMAZAKI

(Received April 27, 1963)

Abstract

The catalytic mechanism, where the recombination of the adsorbed hydrogen atoms determines the rate, predicts the presence of the cathodic saturation current at sufficiently high polarization. The saturation current has been estimated theoretically by HORIUTI as 2×10^{2} A cm^{-2} at 25°C on Ni. The object of the present work was to submit the catalytic mechanism to experimental test by observing the saturation current.

Experiments were carried out on spherical Ni electrode (surface area : 0.01 cm^{2}) in alkaline solutions at 22±1°C. Constant currents ranging from 10^{-3} to 10^{2} A cm^{-2} were applied to the electrode by pulse technique in order to avoid the local heating and concentration polarization at high current densities, which might obscure the experimental results.

Results are as follows. (i) Up to the current density of 1 A cm^{-2}, the TAFEL relation was well established with the slope of 104 or 97 mV and with the exchange current density of 4.7×10^{-6} or 7.9×10^{-6} A cm^{-2} in 0.95±0.02 N or 4.73±0.11 N NaOH solution respectively. The pH effect on these parameters is very small. (ii) Beyond the current density of 1 A cm^{-2}, the overvoltage starts to deviate from the TAFEL relation and increases very rapidly with increase of current density revealing the saturation current. The saturation current was estimated as *ca.* 10^{2} A cm^{-2} in both the solutions. (iii) The values of the exchange current density and the slope were calculated theoretically on the basis of the catalytic mechanism as 2×10^{-6} A cm^{-2} and 100~120 mV ($10^{-4}<i<10^{-1}$ A cm^{-2}) respectively in good agreement with the observed ones.

From these results, it was concluded that the hydrogen evolution reaction proceeds through the catalytic mechanism on Ni electrode in alkaline solutions.

Introduction

A pile of works has been done in various aspects with various methods on the hydrogen evolution reaction,

$$2H^{+}+2e \longrightarrow H_{2}, \qquad (1)$$

where H^{+} is the proton attached to a BRÖNSTED base, $H_{2}O$ or OH^{-}, and e is the metal electron, experimental results being increasingly accumulated with

years. However, the theoretical understandings of these experimental results are still unsettled and controversies are going on between two camps. The one contends the slow discharge mechanism where the rate is governed by the discharge of protons *i.e.*,

$$H^+ + e \overset{A}{\longrightarrow} H(a), \tag{2 a}$$

the adsorbed hydrogen atom H(a) formed being converted into H_2 by the following step either

$$2H(a) \longrightarrow H_2, \quad \text{or} \quad H(a) + H^+ + e \longrightarrow H_2. \tag{2 b}$$

The notation $\overset{A}{\longrightarrow}$ refers to the rate-determining step as in what follows. The other maintains the dual mechanism[1,2] which is an alternative of the catalytic mechanism and the electrochemical mechanism, the operation depending on experimental conditions and electrode material used. The catalytic mechanism causes the hydrogen evolution reaction through the two steps,

$$H^+ + e \longrightarrow H(a), \quad 2H(a) \overset{A}{\longrightarrow} H_2, \tag{3a, 3b}$$

with the rate governed by the latter step and the electrochemical mechanism does similarly through the two steps,

$$2H^+ + e \longrightarrow H_2^+(a), \quad H_2^+(a) + e \overset{A}{\longrightarrow} H_2, \tag{4a, 4b}$$

the rate-determining step being the neutralization of adsorbed hydrogen molecule ion $H_2^+(a)$ formed by the former step.

The slow discharge mechanism has been frequently quoted to be operative by many workers in case where the TAFEL line is of the slope of $2RT/F$[3], since the mechanism leads to the value of $2RT/F$ as well as to a reasonable value of activation energy on the basis of assumption on the equilibrium position of proton to be neutralized, whereas the catalytic mechanism gives $RT/2F$ on the basis of simple classical kinetics. It was shown, however, that the above assumption as regards to the slow discharge mechanism was inadequate and a due consideration led to too small the activation energy for the discharge step to be rate-determining[4], whereas the catalytic mechanism also gives the value near $2RT/F$ by taking the repulsive interaction among adsorbed hydrogen atoms into account[5,6,7] in accordance with the modern theory of adsorption[8,9]. According to the unified theory of dual mechanism[1,2], the catalytic mechanism is responsible for the group of metals such as Ni, Au, Ag, Cu, Pt (at cathodic polarization higher than 0.3 volt in acid solution) and Pb (in alkaline solution), and the electrochemical mechanism for the group of metals Hg, Sn, and Pb (in acid solution) respectively.

The alternative of the slow discharge and the dual mechanisms may be

decided by submitting theoretical conclusions deduced necessarily from them to experimental tests.

Theoretical deductions from the slow discharge mechanism and the dual mechanism with respect to the behaviour of the TAFEL constant, stoichiometric number, separation factor, capacity of an electrode, pH effect, exchange reaction between deuterium gas and water under the presence of electrode material as catalyst *etc.* are distinctly in contrast with each other[7,10]. The followings are particularly referred to the behaviour of the TAFEL constant, $\vec{\tau}$, defined as

$$\vec{\tau} = (RT/F)\,\partial \ln \vec{i}/\partial \eta\,, \qquad (5)$$

with increase of η, where $\vec{i}$ is the forward rate of the reaction (1) in current density and η the overvoltage*). Characteristics of $\vec{\tau}$ for the dual mechanism have been shown that in the case of the electrochemical mechanism, $\vec{\tau}$ changes from 1.5 to 0.5 as η increases so that two linear portions are observed in the TAFEL plot[2,11], whereas in the case of the catalytic mechanism $\vec{\tau}$ changes from 2 to 0 with increase of cathodic polarization staying around 0.5 in accordance with experiments for a considerable range of η[5,6,7]. The coverage of electrode surface with H(a) increases with the polarization through the step (3a) in equilibrium, attaining to its full value at an extremely high polarization, resulting in a constant rate of the rate-determining step (3b), hence $\vec{\tau}=0$. The constant current thus attained will be termed the saturation current. On the other hand, if the slow discharge mechanism is operative, the current can not attain any saturation value with increase of polarization.

It is the object of the present work to follow experimentally the value of $\vec{\tau}$ up to an extremely high cathodic polarization and to decide between the catalytic and the slow discharge mechanism as responsible for the reaction (1) on Ni electrode.

A number of works has been carried out on Ni both in acidic and alkaline solutions[12~19] (see Table 4). However, most of them were concerned in the current densities up to *ca.* 10^{-1} A cm^{-2}, where the TAFEL relations were well established (see Fig. 10). BOCKRIS and AZZAM[15,20] extended the range of current density to 10 A cm^{-2}, taking carefully into account heating effect and concentration polarization at high current densities and observed a positive deviation of the overvoltage from the TAFEL line at 10 A cm^{-2} *i.e.* a tendency of the current to approach a constant value. They concluded, however, the slow discharge mechanism on the ground that the maximum possible current sustained by the catalytic mechanism is *ca.* 1 A cm^{-2}, as estimated from their

*) Overvoltage used in this paper is defined as negative of potential of the test electrode referred to that of the reversible hydrogen electrode in the same solution.

rate expressions. HORIUTI pointed out[21], however, that their expression used was inadequate in dimensions, calculating the maximum possible current in the absence of activation energy at 2×10^{9} A cm^{-2} instead and the saturation current at 2×10^{2} A cm^{-2} at 25°C. The latter theoretical calculation will be discussed briefly in § 1.

§ 1. Theoretical estimation of the saturation current

According to the generalized theory of reaction rate developed by HORIUTI[6,22~24] the forward rate of the hydrogen evolution reaction is given in general as,

$$\vec{i}=\frac{kT}{h}\frac{2F}{\nu(r)N_{\mathrm{A}}}\frac{\exp(-\mu_r^*/RT)}{\exp(-\mu_r^{\mathrm{I}}/RT)}, \tag{6}$$

where $\nu(r)$ is the stoichiometric number of rate-determining step r, μ_r^* or μ_r^{I} is the chemical potential of the activated state or the initial state of the step r respectively and k, T, h, F, N_{A} and R have the usual meanings. Assuming the catalytic mechanism, hence $\nu(r)=1$, $\mu_r^{\mathrm{I}}=2\mu^{\mathrm{H(a)}}$, where $\mu^{\mathrm{H(a)}}$ is the chemical potential of H(a), Eq.(6) becomes

$$\vec{i}=\frac{kT}{h}\frac{2F}{N_{\mathrm{A}}}\frac{\exp(-\mu^*/RT)}{\exp(-2\mu^{\mathrm{H(a)}}/RT)}. \tag{7}$$

The chemical potentials, μ^* and $\mu^{\mathrm{H(a)}}$, are expressed as[5,22],

$$\mu^*=-RT\ln\frac{\Theta_{\sigma^*(\mathrm{O})}}{\Theta_{\sigma^*(*)}}+U^*+\varepsilon_0^*, \tag{8}$$

and

$$\mu^{\mathrm{H(a)}}=-RT\ln\frac{\Theta_{\sigma(\mathrm{O})}}{\Theta_{\sigma(\mathrm{H})}}+U^{\mathrm{H(a)}}+\varepsilon_0^{\mathrm{H(a)}}, \tag{9}$$

where $\Theta_{\sigma^*(\mathrm{O})}$ or $\Theta_{\sigma^*(*)}$ is the probability of σ^*, the site for the activated state, being vacant or occupied by the activated state $*$, $\Theta_{\sigma(\mathrm{O})}$ or $\Theta_{\sigma(\mathrm{H})}$ is also the probability of σ, the site for the hydrogen atom, being vacant or occupied by a hydrogen atom, U^* or $U^{\mathrm{H(a)}}$ is the potential of repulsion exerted upon $*$ or H(a) by surrounding adsorbed hydrogen atoms and ε_0^* or $\varepsilon_0^{\mathrm{H(a)}}$ is the reversible work required to bring $*$ or hydrogen atom from the respective standard states of their components into a definite site σ^* or σ respectively in the absence of repulsion. $\Theta_{\sigma^*(\mathrm{O})}$ *etc.* were expressed in the theory assuming that H(a) is only predominant occupant on the surface and that repulsive potentials are respectively proportional to $\Theta_{\sigma(\mathrm{H})}$, as[21]

$$\left.\begin{aligned} &\Theta_{\sigma^*(*)} = 1/G, \quad \Theta_{\sigma^*(\mathrm{o})} = (1-\theta)^2 \Big/ \left[1+\theta\left\{\exp\left(\frac{u_1\theta}{RT}\right)-1\right\}\right], \\ &\Theta_{\sigma(\mathrm{H})} = \theta, \quad \Theta_{\sigma(\mathrm{o})} = (1-\theta), \end{aligned}\right\} \tag{10}$$

where θ is the covered fraction of the surface with H(a), G the number of σ^* on the surface per unit area and u_1 the repulsive potential between two H(a)'s situated on the adjacent sites constituting σ^*. Using Eqs. (8), (9) and (10), Eq. (7) is rewritten as,

$$\vec{i} = \frac{kT}{h}\frac{2F}{N_A}G\frac{\theta^2}{1+\theta\left\{\exp\left(\frac{u_1\theta}{RT}\right)-1\right\}}\exp\left(\frac{2U^{\mathrm{H(a)}}-U^*}{RT}\right)\exp\left(\frac{2\varepsilon_0^{\mathrm{H(a)}}-\varepsilon_0^*}{RT}\right). \tag{11}$$

Eq. (11) gives the saturation current $\vec{i}_{\theta=1}$ *i.e.*, $\vec{i}$ at the condition $\theta=1$, as

$$\vec{i}_{\theta=1} = \frac{kT}{h}\frac{2F}{N_A}G\exp\left(\frac{2u^{\mathrm{H(a)}}-u^*-u_1}{RT}\right)\exp\left(\frac{2\varepsilon_0^{\mathrm{H(a)}}-\varepsilon_0^*}{RT}\right), \tag{12}$$

where $u^{\mathrm{H(a)}}$ or u^* is the repulsive potential $U^{\mathrm{H(a)}}$ or U^* at $\theta=1$ respectively. $u^{\mathrm{H(a)}}$, u^* and u_1 were calculated semiempirically as 25.0, 34.7, and 1.4 kcal mole^{-1} respectively using the experimental values for the heat of adsorption of hydrogen on Ni obtained by KWAN.[25,26] $2\varepsilon_0^{\mathrm{H(a)}}-\varepsilon_0^*$ was similarly evaluated as -11 kcal mole^{-1} from the limiting value of the heat of adsorption at $\theta\to 0$. With these numerical values and 10^{15} cm^{-2} for G[5], the saturation current was estimated at 2×10^2 A cm^{-2} at 25°C.

It would be noted in the above calculation that the heat of adsorption used is that obtained in the system of hydrogen gas and Ni in the absence of water. This is justified, if H(a)'s do not interact significantly with water or ionic species on the solution side of double layer. If the same is the case with the activated state, so that $u^{\mathrm{H(a)}}$ *etc.* and $\varepsilon_0^{\mathrm{H(a)}}$ *etc.* in Eq. (12) will remain unchanged with pH, the saturation current does not depend on the pH of solution as seen from Eq. (12).

The value of saturation current is now submitted to experimental test at different concentrations of NaOH.

§ 2. Experimental

Experiments at high current densities will be associated with difficulties due to heating effect and concentration change near electrode. These difficulties were overcome by using short pulse of a constant current. Although drifts of the overvoltage at a constant applied current for an hour on Ni have been reported, appropriateness of rapid measurements by the pulse method, has been confirmed by most reproducible results obtained[14,27].

Experimental methods are similar to that used by BOCKRIS *et al*[28,29].

The apparatus

The apparatus illustrated in Fig. 1 schematically comprises purification units for gases, device for preparing electrode, cell, pulse generator and recorder of potential of electrode. The glass used was the borosilicate glass called Hario of SHIBATA & Co., Tokyo.

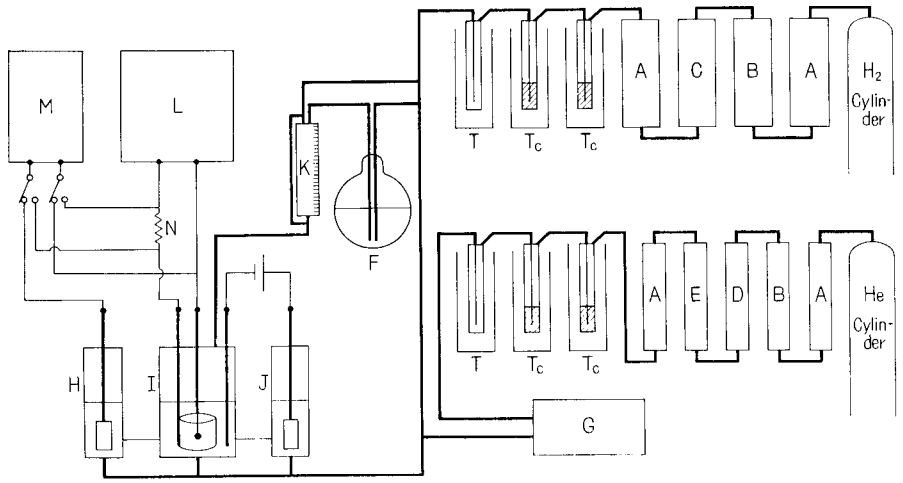

Fig. 1. Schematic diagram of the apparatus

A: Silicagel, B: Soda lime, C: Pt asbestos heated at about 350°C, D: Hopcalite, E: Cu heated at about 600°C, F: Storage of the electrolyte solution, G: Device for the preparation of spherical electrode, H: Reference compartment, I: Main compartment, J: Anode compartment, K: Graduated cylinder, L: Pulse generator, M: Cathode ray oscilloscope, N: Standard resistance (10 or 100 ohms), T: Liq. N_2 cooled trap, suffix c indicates to contain active charcoal.

The purification units: Hydrogen from cylinder was purified through a train consisting of columns of silicagel (A in Fig. 1), soda lime (B), platinum asbestos heated at about 350°C (C), silicagel and three liquid N_2 cooled traps, the first two of them containing tablets of active carbon. He-gas was purified similarly with additional columns of hopcalite (D) and copper heated at about 600°C (E) instead of the platinum asbestos. In order to prevent any contamination by organic compounds, taps used were all greaseless. Water used for final washing of the cell and for the preparation of electrolyte was produced in a still containing alkaline $KMnO_4$ solution. Conductivity of the water thus obtained was less than 10^{-6} mhos cm^{-1} (called the conductivity water in what follows).

Electrolyte solutions: Special grade of NaOH from KANTO Chem. Co., Tokyo, was used. Concentrations were 0.95 ± 0.02 N and 4.73 ± 0.11 N (*cf.* Table 2). These were kept in the flask (F in Fig. 1) in atmosphere of hydrogen purified as above.

Electrodes: The electrodes were spheres of nickel prepared in G in Fig. 1 by melting thin

wire of purity 99.99% from JOHNSON, MATHEY & Co., London, (0.1 mm dia., 1.3 cm length) in purified He, the surface having been previously freed from oxide by reduction in hydrogen purified as above at elevated temperatures. The sphere was sealed into thin walled glass bulb with the sample of hydrogen in order to prevent a contact of the surface with air. Surface area of the electrode was calculated as a sphere of the mean diameter of the least and the greatest ones as observed with comparator after the experiments (about 0.01 cm^2, see Table 2).

Cell: The cell was similar to that used by BOCKRIS *et al.*[14,29,30] It consisted of reference, main and anode compartments (H, I, J in Fig. 1). Detailed features are shown in Fig. 2. The main compartment could hold six electrodes sliding through slip joints in the top of the cap. One of these electrodes is the counter electrode (E_1 in Fig. 2) of platinized cylindrical platinum net, another is the cathode of platinum wire (E_2) for the pre-electrolysis. The rests are the

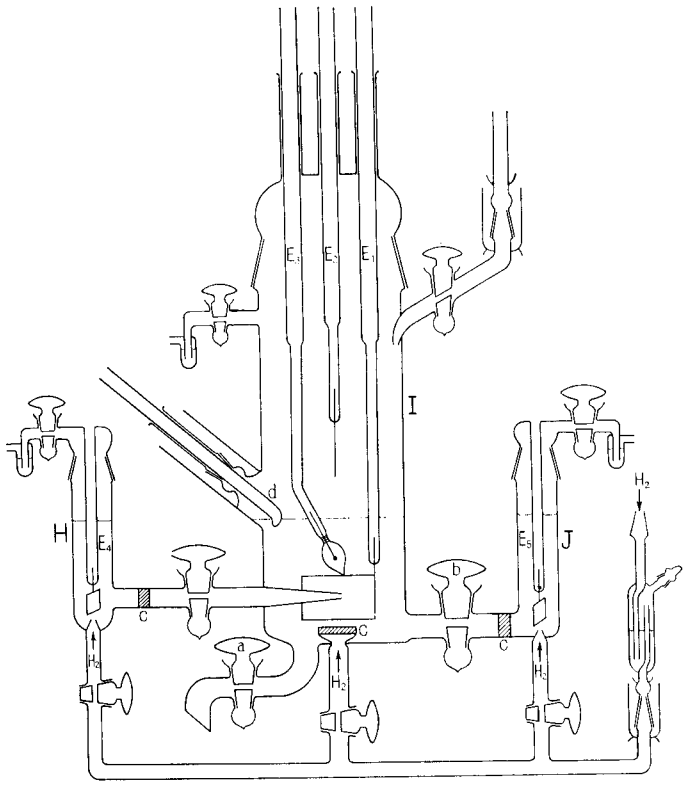

Fig. 2. Cell diagram

H: Reference compartment, I: Main compartment, J: Anode compartment, a, b: Taps, c: Sinterd glass disk, d: Glass bar for breaking the thin glass bulb of the test electrode, E_1: Counter electrode, E_2: Cathode for pre-electrolysis, E_3: Test electrode, E_4: Reference electrode, E_5: Anode for pre-electrolysis.

test electrodes, only one of them being shown in the Figure (E_3). Reference electrode (E_4) and anode used in pre-electrolysis (E_5) were platinized platinum foil. These compartments were connected with sintered glass disks c.

Pulse generator: The circuit of pulse generator is shown in Fig. 3. The arrangement is the similar to that of MEHL, DEVANATHAN and BOCKRIS[31] and BOCKRIS and KITA[29]. The length of pulse was controllable over the wide range from 0.1 msec to sec. The pulses longer than 0.1 sec were obtained by closing the microswitch M by putting switches, S_1 in the position of dotted line and S_2 in off position. The shorter pulses up to msec were obtained by controlling the variable condenser C_1 with S_1 in the position of full line and S_2 in the off position. The pulses from msec to 0.1 msec. were obtained by the operations of the variable

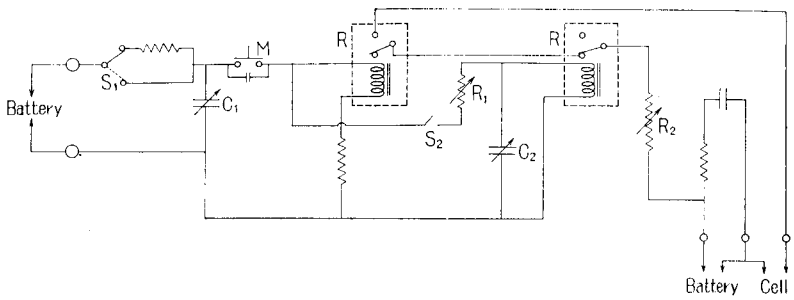

Fig. 3. Electric device for producing pulses
M: Microswitch, S: Switches, C: Variable condensers for controlling pulse duration, R_1: Variable resistance for controlling pulse duration, R_2: Variable resistance for controlling current density, R: Relays of Western Electric Co. 275 B., U.S.A.

resistance R_1 and the variable condensers C_1 and C_2, with S_1 in the position of full line keeping S_2 on. R is the relays of Western Electric 275B, U.S.A. A current supplied to the electrodes was kept constant passing it through the variable resistance R_2 high enough that the resistance of the cell amounts to within 1% of the all. Maximum current obtained was 1 A. Rise time of the pulses was less than 2 μsec at the current from mA to 1 A and increases with decrease of current but was less than msec even at the lowest current 10 μA used. Sharp cutting off the current was not effected for currents higher than 0.2 A (*cf.* Fig. 6(c)).

Recorder of potential: Potential-time curves for applied currents were recorded on the screen of the cathode ray oscilloscope (Synchroscope SS 5302, Preamp, SP-15H-A, IWASAKI Communication Apparatus Co., LTD. Tokyo).

Procedure

Before the experiments, the cell and the bulbs of the test electrodes were cleaned overnight with a mixture of 50–50 concentrated nitric and sulphuric acid. The cell, the bulbs containing spherical electrodes and the counter electrode freshly platinized before every series of experiments were washed thoroughly with the conductivity water, with particular care to remove any trace of acid from the sintered glass disks.

A series of experiments was conducted as follows. Electrodes were mounted by their upper cylindrical part on the cap of the cell, the cell was filled up with the conductivity water and set in the apparatus as in Fig. 1. A few hours later, the water in the cell was pushed

out through tap a in Fig. 2 by pressure of the purified hydrogen and an electrolyte solution of a desired composition was introduced from the graduated cylinder K (Fig. 1) similarly by hydrogen pressure. The solution first introduced was discarded after being transferred several times from one to other among three compartments to replace water remaining in the cell with the solution. The solution is subsequently introduced by *ca.* 100 cc., for the experiments. The concentration of solution, *i.e.* $NaOH_{aq}$ was 0.95 ± 0.02 N or 4.73 ± 0.11 N on an average (*cf.* Table 2). Pre-electrolysis was now conducted bubbling hydrogen for 2~3 days with current 3.5 mA using the electrodes E_2 and E_5, separating the latter from the main compartment by the closed tap b and the sintered glass disk. Further prolonged electrolysis did not affect experimental results. After pre-electrolysis, one of the test electrodes was slided down and its glass bulb was fractured by glass bar d in Fig. 2. The exposed sphere of test electrode in solution was positioned just in front of the tip of LUGGIN capillary which was centered in the cylindrical counter electrode. Single pulses of a constant current were imposed on the test electrode, while the resulting potential changes were revealed on the screen of the cathode ray oscilloscope. The potentials were always referred to that of the reversible hydrogen electrode in the same solution. A series of potential-time curves was photographed on film (Neopan SSS, Fuji photo Film Co. LTD) with a camera (Canon RM. F, 1.2) over the current density ranging from 10^{-3} to 10^{2} A cm^{-2}. The constant current was accurately estimated by measuring the potential drop across the standard resistance, N in Fig. 1, of 10 or 100 ohms in the cell circuit using the same oscilloscope. The current was usually changed from low to high ones and occasionally back again. The films were enlarged 15-fold for analyses.

Solutions were titrated with standard HCl (1.0 N) solution after the experiments. Experiments were all carried out at 22 ± 1°C.

The duration of pulses

At high current densities, the duration of pulses has to be shortened to avoid the heating effect and the change of concentration near the electrode.

Appropriate duration of pulses was determined considering the possible maximum temperature rise of the electrode surface during the pulse and the possible maximum concentration change.

Heating effect: Assuming that the heat evolved during the reaction is absorbed only by the spherical electrode, a rise in temperature, T, was calculated as below as a function of the time of duration and current density. The appropriate differential equation is given, assuming isotropic heat transfer and homogeneous thermal conductivity throughout the body of electrode, as,

$$\frac{\partial T}{\partial t}=\frac{\kappa}{\rho c}\left(\frac{\partial^2 T}{\partial r^2}+\frac{2}{r}\frac{\partial T}{\partial r}\right), \tag{13}$$

where t is the time, κ the specific conductivity of heat, ρ the density, c the specific heat and r the distance from the center of sphere. Using the initial and boundary conditions, that the initial temperature, T_0, is uniform in the sphere at $t=0$ and that the amount of heat transferred in unit time, F_0, is constant at the surface ($r=a$), *i.e.*,

$$T = T_0, \qquad a > r > 0 \text{ and } t = 0$$

$$F_0 = \frac{\kappa}{\rho c}\left(\frac{\partial T}{\partial r}\right) = \text{const.}, \qquad r = a, \text{ and } t > 0.$$

Eq. (13) is integrated as[32],

$$T_t - T_0 = \frac{F_0 \rho c a}{\kappa}\left\{\frac{3\kappa t}{\rho c a^2} + \frac{r^2}{2a^2} - \frac{3}{10} - 2\frac{a}{r}\sum_{n=1}^{\infty}\frac{\sin(\alpha_n r)}{\alpha_n^2 a^2 \sin(\alpha_n a)}\exp\left(-\frac{\kappa}{\rho c}\alpha_n^2 t\right)\right\}, \tag{14}$$

where the $\alpha_n a$'s are the positive roots of $\alpha_n a \cot \alpha_n a = 1$. F_0 is given in terms of the constant current density i and the overvoltage η*) as

$$F_0 = \frac{i}{2F}(2F\eta + T\Delta S), \tag{15}$$

where ΔS is the increment of entropy of the reaction (1) ($T\Delta S = 2.16$ kcal mole^{-1} at 1 molal OH^-, 1 atm H_2 and 23°C)[33]. Using numerical values as $\rho = 8.9$ g cm^{-3}[34], $c = 0.11$ cal^{-1} g^{-1}[35], $a = 0.03$ cm and $\kappa = 0.2$ cal sec^{-1} cm^{-2} deg^{-1}[36] for Ni, the time τ at which the temperature rise at the electrode surface amounts to 2°C was calculated at various high current densities as shown in Table 1. The temperature rise thus calculated is the maximum possible one, since the heat evolved may be absorbed by the solution as well.

Concentration change near the electrode: A change in concentration near the electrode surface is similarly estimated by the differential equation,

TABLE 1. Duration of pulses at high current densities
τ : The time at which the temperature of the electrode surface rises 2 degree
η_c : Concentration polarization

i (A cm^{-2})	80	29	21	14	10
η (volt)	2.0	1.3	1.1	1.0	0.95
τ (msec)	~0.1	~1	~2	~3	~4
η_c (OH^-)	~0.02 V				
η_c (H_2)	0.08~0.09 V**)				

*) See the footnote on p. 12

**) See the footnote **) on p. 20

$$\frac{\partial C}{\partial t} = D\left(\frac{\partial^2 C}{\partial r^2} + \frac{2}{r}\frac{\partial C}{\partial r}\right), \tag{16}$$

assuming the reaction products OH^- or H_2 to leave the surface only through diffusion, where C is the concentration and D the diffusion coefficient of OH^- or H_2. Using the conditions,

$$C = C_0, \qquad r > a \quad \text{and} \quad t = 0$$

$$-D\left(\frac{\partial C}{\partial r}\right) = \frac{i}{zF} = \text{const}, \qquad r = a \quad \text{and} \quad t > 0$$

$$C = C_0, \qquad r = \infty \quad \text{and} \quad t \geqslant 0$$

Eq. (16) is integrated as

$$C_t - C_0 = \frac{a^2 i}{DzF}\left[-\exp\left(\frac{r-a}{a}\right)\exp\left(\frac{Dt}{a^2}\right)\operatorname{erfc}\left(\frac{\sqrt{Dt}}{a} + \frac{r-a}{2\sqrt{Dt}}\right) + \operatorname{erfc}\left(\frac{r-a}{2\sqrt{Dt}}\right)\right]. \tag{17}$$

From the respective values for i, D and τ, $C_{r=a}$'s and hence the concentration polarizations defined as $(RT/zF)\ \ln\ (C_{r=a}/C_0)$, were calculated on the base of $D = 5.2 \times 10^{-5}\ \text{cm}^2\ \text{sec}^{-1}$*) or $D = 5 \times 10^{-5}\ \text{cm}^2\ \text{sec}^{-1}$[38] and $z = 1$ or 2 for OH^- or H_2 respectively as shown in Table 1. These values are negligibly small as compared with the observed high overvoltages within experimental errors at the high current densities. Calculated values may be the upper bound to the actual ones owing to the stirring of solution by bubbling the hydrogen from the purification unit in the present experimental conditions**).

The duration of pulses at these high current densities was hence kept within τ shown in Table 1.

Estimation of overvoltage, η***)**

Measured potential comprises the overvoltage and the potential due to the solution resistance (called *IR* drop) between the tip of LUGGIN capillary and the spherical electrode. Actually the potential rose instantaneously on setting in of a constant current and then linearly with much slower rate attaining

*) Diffusion coefficient of OH^- was calculated from the EINSTEIN's diffusion equation, $D = \frac{RT}{z^2F^2} l_\infty$, using numerical value for l_∞, the mobility of OH^- at infinite dilution, as 198 $\text{cm}^2\ \text{ohm}^{-1}$ at 25°C[37].

**) According to CLARMROTH and KNORR[39], the concentration of H_2 in solution cannot exceed 0.04 mol l^{-1} because of bubble formation which corresponds to the solubility at 10~100 atmospheric pressures *i.e.*, 30~60 mV in the concentration polarization.

***) See the footnote on p. 12

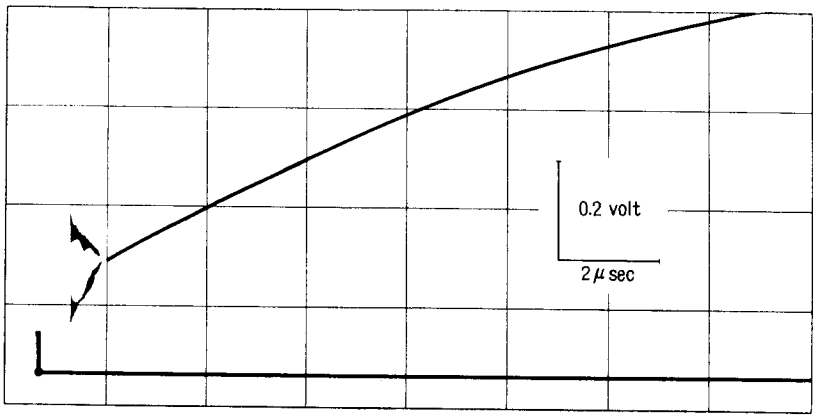

Fig. 4. Rapidly swept potential-time curve
Current density: 3.24 A cm^{-2}, Solution: 4.91 N NaOH,
Temp.: 22°C

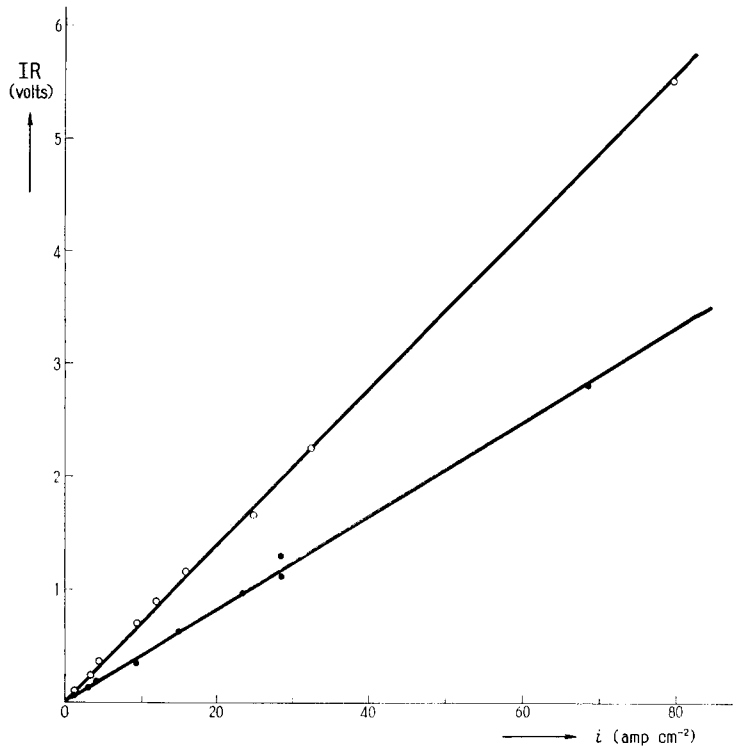

Fig. 5. Relation between the *IR* drop and the current density
○: 0.95 N NaOH solution, ●: 4.63 N NaOH solution,
Temp: 22°C

finally to a constant value as observed with high sweeping rate as shown in Fig. 4. The *IR* drop was estimated by extrapolating the linear part at $t=0$. The *IR* drop thus determined is proportional to the current density, as expected, both in 0.95 ± 0.02 N and 4.73 ± 0.11 N NaOH solutions as illustrated in Fig. 5. Overvoltages were determined by subtracting *IR* drop extrapolated at $t=0$ at a given current density from the observed potential.

§ 3. Results

Rest potential

Rest potential of a test electrode was measured by the oscilloscope before and after the experiments as referred to that of the reversible hydrogen electrode in the same solution. Results are shown in Table 2. Electrodes of a rest potential amounting a few hundred millivolts gave unusual η--log i relation, which were discarded.

Transients

Typical transients at low, intermediate and high current densities are shown in Fig. 6. The potential increases with time at the beginning and approaches a constant value, *i.e.* the steady state is attained. At low current densities ($i<10^{-1}$ A cm^{-2}), a superpolarization occurs and its peak value exceeds the steady potential as much as *ca.* 30 mV at the lowest current density applied. Any systematic variation of the excess values was not observed by changing either the concentration of NaOH from 1 N to 5 N or the time of pre-electrolysis from 2 to 3 days. The superpolarization becomes less pronounced with increase of current density and imperceptible at intermediate current densities (Fig. 6, b) and above. At high current densities, however, the first rapid settling of potential is followed with a gradual increase of it with time as shown in Fig. 6, c. When long pulse of the highest current density, order of msec, is applied, the potential rises after the first rapid settling, apparently to approach a few volts higher value, which fluctuates considerably irregularly. Duration of the highest current density for *ca.* 100 msec. makes the electrode dark red-hot. The potential of first settling was taken as steady state value for the hydrogen evolution reaction on the ground described later.

Capacity, C_E, of the electrode was estimated from the very initial rise of potential according to the equation,

$$C_E = i \Big/ \left(\frac{\partial \eta}{\partial t}\right)_{t=0}$$

at various current densities. The capacity thus determined decreases slightly

TABLE 2. Experimental conditions and Results.
Temperature : 22±1°C

Concentration of NaOH (N)		Diameter of electrode (mm)	Surface area (cm^2)	Rest potential of test electrode referred to the reversible hydrogen electrode (mV) befor	after	Exchange current density ($A\,cm^{-2} \times 10^{-6}$)	Slope of the TAFEL line (mV)	Capacity ($\mu F\,cm^{-2}$)
1	0.94	0.526 0.629	0.011	− 6.0	− 3.2	3.4	128	24
2	0.94	0.546 0.550	0.011	−13.0	0.0	2.5	118	36
3	0.93	0.485 0.739	0.012			0.4	105	53
4	0.93	0.457 0.465	0.0067	13.5	− 1.5	1.5	107	32
5	0.96	0.543 0.553	0.0094	17.0	− 3.7	4.3	96	124
6	0.96	0.553 0.561	0.0097	− 2.5	− 0.7	2.9	100	57
7	0.98	0.556 0.579	0.010	16.0	17.0	2.2	98	52
8	0.98	0.492 0.700	0.011	13.0	1.5	1.0	100	35
9	0.95	0.542 0.555	0.0094	1.8	− 7.0	16	99	75
10	0.95	0.542 0.573	0.0097	−29.0	−25.0	13	90	165
Mean	0.95± 0.02N		0.010 ±0.001			4.7	104±9	65
1	4.63		0.010	29.0	28.0	1.8	93	88
2	4.63		0.0094	2.0	10.0	25	100	116
3	4.76		0.0090	−15.0	0.0	1.6	85	82
4	4.61	0.473 0.821	0.013	− 3.5	− 3.0	1.7	90	46
5	4.61	0.523 0.753	0.013			1.7	96	74
6	4.77	0.546 0.572	0.0097	− 2.3	− 1.8	4.6	102	49
7	4.91	0.534 0.545	0.0093	−30.0	−25.0	10	105	48
8	4.93	0.502 0.540	0.0082	0.3	− 1.4	17	101	170
Mean	4.73 ±0.11N		0.010 ±0.002			7.9	97±5	84

with decrease of current density (Fig. 7) and tends to approach a constant value which was shown in Table 2 for each electrode.

Steady State

The $\eta-\log i$ relations at the steady state in NaOH solutions of concentrations 0.95 ± 0.02 N and 4.73 ± 0.11 N respectively are presented in Figs. 8 and 9. The well-known TAFEL relation holds very well up to the current

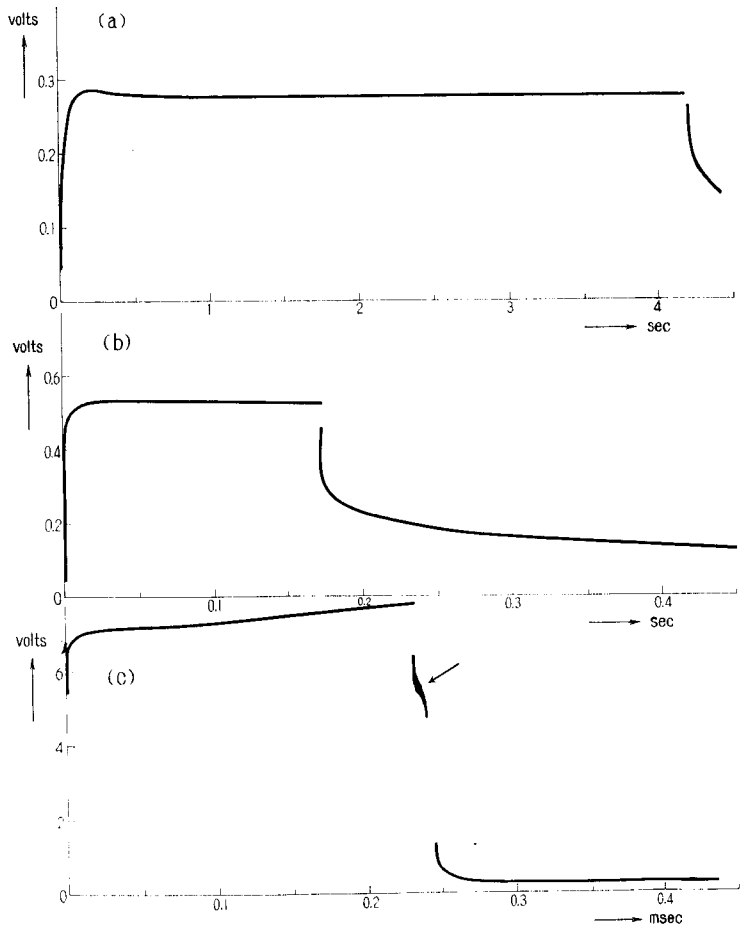

Fig. 6. Typical transients at low, intermediate and high current densities (a) $i=9.3\times10^{-3}$ A cm^{-2}, (b) $i=5.2\times10^{-1}$ A cm^{-2}, (c) $i=80$ A cm^{-2}, Solution: 0.95 N NaOH, Temp: 22°C, Surface area: 0.0094 cm^2
Trace pointed out with arrow in (c) is due to chatterring occurred at cutting off the current.

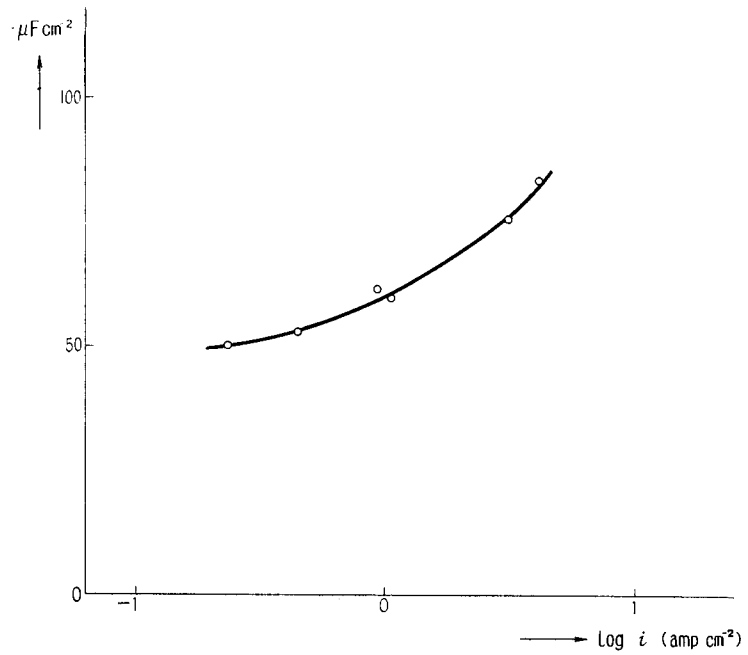

Fig. 7. Differential capacity at various current densities
Solution: 4.8 N NaOH, Temp: 22°C, Surface area: 0.0097 cm^2

density of 1 A cm^{-2}, appropriate slope, b, and the exchange current density, i_0, *i.e.* the extrapolation of the i according to the TAFEL relation at $\eta=0$ being summerized in Table 2. The pH effect on i_0 is almost zero within experimental errors. The b-value is smaller in 4.73 ± 0.11 N solution than in 0.95 ± 0.02 N solution by 7 mV on an average.

Beyond the current density of 1 A cm^{-2}, overpotential starts to deviate positively from the TAFEL line and increases quite rapidly in the range of 10～100 A cm^{-2} amounting to a few volts. Such a large increase of η verifies the presence of the saturation current. Its value may be taken safely as about 100 A cm^{-2} in alkaline solution of both the concentrations.

The η was observed reproducibly within 5% by changing the current from low to high and then reversely from high to low but different electrodes of the same preparation gave results not so reproducible as in the above case with one and the same electrode. The activity of the sphere electrode in terms of the magnitude of the exchange current was found greater in 4.73 ± 0.11 N solution than in 0.95 ± 0.02 N conducted earlier by about 2 factor, whereas the activity of the sphere electrode of later preparation was found in general

enhanced to the same extent as compared with those of earlier preparation even in one and the same solution.

§ 4. Discussion

Reaction Mechanism

As described above, the saturation current was experimentally confirmed and its observed value of *ca.* 100 A cm^{-2} is very close to that predicted from the catalytic mechanism. Hence the mechanism of the hydrogen evolution

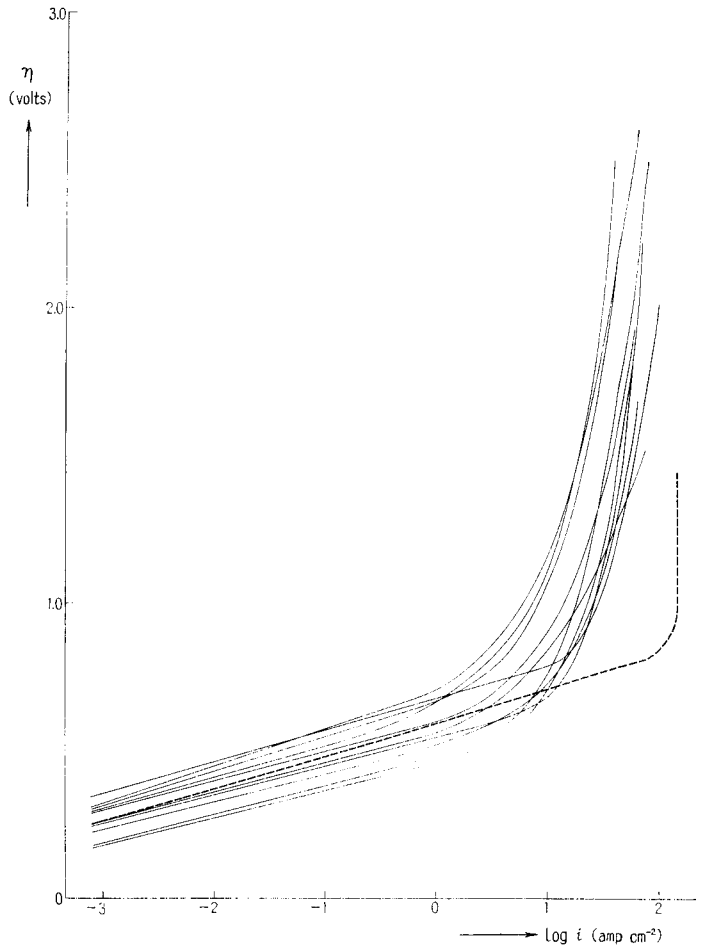

Fig. 8. Relationship between the overvoltage and log i in the solution of 0.95±0.02 N NaOH at 22±1°C
Dotted line is the calculated one from Eq. (11).

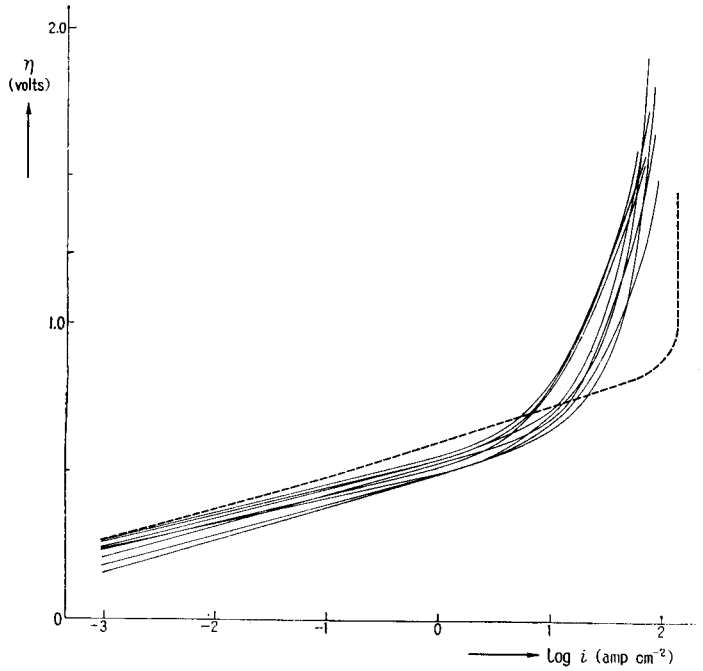

Fig. 9. Relationship between the overvoltage and log i in the solution of 4.73±0.11 N NaOH at 22±1°C
Dotted line is the calculated one from Eq. (11).

reaction on Ni in alkaline solution is concluded as the catalytic one, hence the recombination of adsorbed hydrogen atoms governs the overall reaction rate. This conclusion can be further supported by the insignificant pH effects on the values of saturation current and exchange current.

The same conclusion has been arrived at recently in this Institute on Ni electrode. MATUDA and OHMORI[18,19] have found very large differential capacity attaining a maximum at around 50 mV of η, which amounts to 1000～1700 μF per unit apparent area, and very small pH dependence of η at a constant current density on the evapolated film electrode in alkaline solutions. The large capacity with a maximum is the necessary conclusion from the catalytic mechanism, *i.e.* that due to H(a) in equilibrium with protons and electrons[40-42] and the very small pH effect is another, that derived from the rate-determining recombination. ENYO, HOSHI and one of present authors[43] conducted the exchange reaction between deuterium gas and aqueous alkaline solutions on Ni wire at various pH's and deuterium pressures at 0～50°C. They found no dependence of the rate of exchange effected by hydrogen electrode reaction upon pH, which verifies the above conclusion.

Slope of TAFEL line and exchange current density

As mentioned in the introduction, a number of workers maintains the slow discharge mechanism as being operative on Ni mainly on the ground that the observed b-value is close to $2RT/F$. It may be noted that the quantum mechanical picture on the basis of the slow discharge mechanism which accounts for this value of b, fails on the other hand to explain the observed magnitude of activation energy of hydrogen evolution reaction[4,10]. It is shown below that the observed b-value can be explained also by the catalytic mechanism, while the magnitude of activation energy mentioned above is deduced reasonably from the latter mechanism[4,10]. The $\eta-\log\vec{i}$ relation is given theoretically by Eq. (11) on the basis of the catalytic mechanism, where θ is determined as a function of η on account of the appropriate equilibrium of the step, $H^+ + e \rightarrow H$ (a), as[5,21,44],

$$\theta = [1+\exp\{(\varepsilon_0^{H(a)} + u^{H(a)}\theta - \tfrac{1}{2}\mu^{H_2} - F\eta)/RT\}]^{-1} \qquad (18)$$

The values of θ at various η's are calculated using numerical values for $\varepsilon_0^{H(a)}$, $u^{H(a)}$ and μ^{H_2} (see §1) as shown in Table 3. With these values and Eq. (11), $\eta-\log\vec{i}$ relationship is calculated, assuming the proportionality of repulsive potentials to θ, as shown by dotted lines in Figs. 8 and 9.

TABLE 3. Coverage of H(a) on Ni electrode surface at various overvoltages calculated from Eq. (18) at 25°C

η/59.1 mV	0	1	2	3	4	6	8	10	14
θ	0.31	0.36	0.41	0.46	0.51	0.61	0.71	0.80	0.97

The slope is 100~120 mV over the range of current density, $10^{-4} < i < 10^{-1}$ A cm^{-2}, which is in good agreement with the observed b values (Table 2). Exchange current density is calculated from Eqs. (11) and (18) putting $\eta=0$ at 2×10^{-6} A cm^{-2} which is in reasonable agreement with the experimental values of i_0 in consideration of accuracy of their extrapolation by TAFEL lines.

It can be seen from the above mentioned consistency between the theoretical and the observed values that the presence of water would not significantly affect the heat of adsorption of hydrogen on Ni, the heat of adsorption used in the above calculation being that derived from the observed adsorption isotherm of gaseous hydrogen onto Ni powder in the absence of water.

Comparison of the present experimental results with those in literature

The i_0 and b values in the present work are compared with the literature

TABLE 4. Comparison of the present results with others

Workers	Solution	Temperature	i_0 (A cm^{-2})	b (mV)
Present work	0.95 N NaOH	22°±1°C	4.7×10^{-6} (calc. 2×10^{-6})	104 (calc. 100~120 at $10^{-4}<i<10^{-1}$)
	4.73 N NaOH		7.9×10^{-6}	97
BOCKRIS and POTTER[14]	0.1 N NaOH	20°C	4×10^{-7}	101
	0.006 N NaOH		2.5×10^{-7}	101
	0.001 N NaOH		1×10^{-7}	103
	1.0 N HCl		4×10^{-6}	109
	0.1 N HCl		1×10^{-6}	104
	0.01 N HCl		2×10^{-7}	91
	0.001 N HCl		2.5×10^{-7}	93
LUKOVSEV, LEVINA and FRUMKIN[13]	0.0003 N HCl		2×10^{-7}	90
	0.0012 N HCl		2×10^{-7}	90
	0.013 N HCl		3×10^{-7}	100
	0.15 N HCl		1×10^{-6}	100
BOWDEN and RIDEAL[12]	0.2 N H_2SO_4	25°C	2.5×10^{-7}	110
JEFFERYS, YEAGER and HOVORKA[8]	0.02 N H_2SO_4	25°C	4×10^{-7}	110
	0.1 N H_2SO_4		5×10^{-7}	95
	1 N H_2SO_4		3×10^{-5}	97
CONWAY, BEATTY and DEMAINE[16]	0.1 N HCl	38°C	7×10^{-6}	96
MAKRIDES[17]	0.1 N NaOH	30°C	$0.7\sim1.2\times10^{-5}$	90~93
MATUDA and OHMORI[18,19]	pH 13.68 NaOH	20°C	8.9×10^{-6}	90
	pH 12.68 NaOH		7.9×10^{-6}	95
	pH 11.92 NaOH		7.4×10^{-6}	100
	pH 10.72 NaOH		5.6×10^{-6}	110
ENYO, HOSHI and KITA[43]	pH=7.4~13, NaOH	30°C	*ca.* 2×10^{-6}	

values in Table 4. Tafel lines are shown in Fig. 10. Comparison shows (i) that our results are in harmony with others and (ii) that pH effect on i_0 is small as found in the present work in conformity with results in literature, which is only understandable on the basis of the catalytic mechanism.

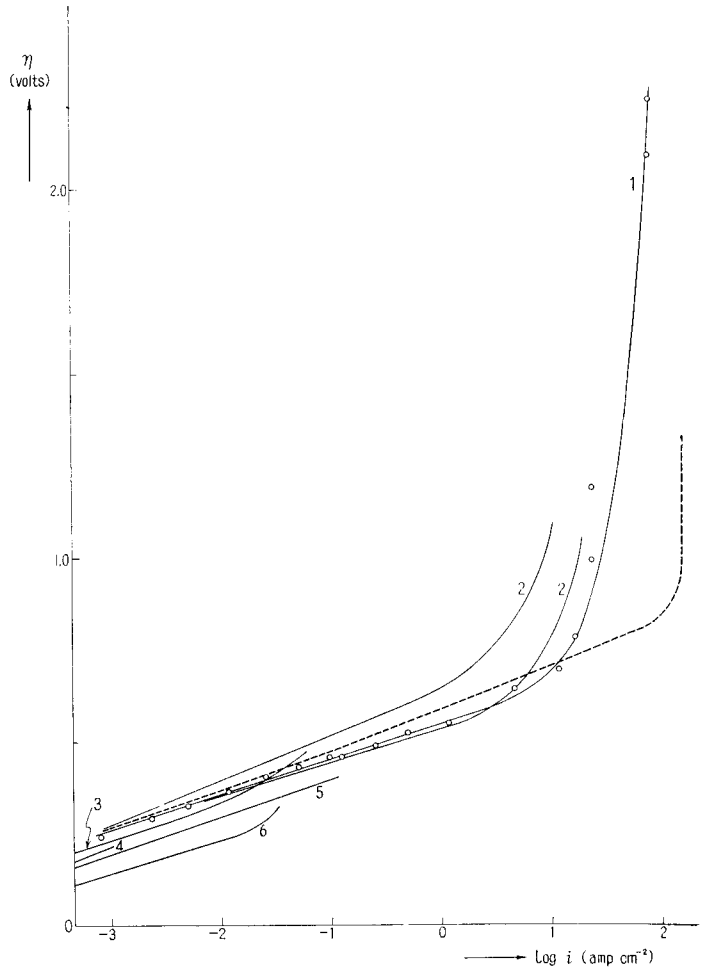

Fig. 10. Comparison of the present results with others
1: Present result (0.955 N NaOH, 21°C), 2: BOCKRIS and AZZAM[15] (5 N HCl), 3: MATUDA and OHMORI[18,19] (pH 10.72~13.68 NaOH 20°C), 4: MAKRIDES[17] (0.1 N NaOH, 30°C), 5: CONWAY, BEATTY and DEMAINE[16] (0.1 N HCl 38°C), 6: YEAGER[45] (1.0 N H_2SO_4 25°C), Dotted line is the calculated one from Eq. (11).

Possibility of sodium electrode reaction

Finally, the possibility of sodium electrode reaction will be discussed briefly. The reversible potential of the sodium electrode reaction,

$$Na^+ + e \longrightarrow Na\,, \qquad (19)$$

is known as -2.714 V[33] as referred to the normal hydrogen electrode potential, at 1 molal concentration of Na^+ and 25°C. In the present experimental conditions, the reversible potential of the hydrogen electrode in 1 N NaOH is close to -0.828 V (1 molal NaOH, 25°C) as referred to the normal one, hence at overvoltage exceeding *ca.* 1.9 V, a deposition of sodium could possibly occur. Two competing reactions (1) and (19) might have resulted in the complicated phenomenon of the gradual increase of η at high current densities.

Conclusive remarks

(1) The cathodic saturation current was observed experimentally on Ni in 0.95 ± 0.02 N and 4.73 ± 0.11 N NaOH solutions at 22 ± 1°C.

(2) The value of the saturation current was determined as about 10^2 A cm^{-2} which is very close to the theoretically predicted value of 2×10^2 A cm^{-2} at 25°C.

(3) The effects of pH on the saturation current and the exchange current were found insignificant. Exchange current density is observed as 4.7×10^{-6} A cm^{-2} or 7.9×10^{-6} A cm^{-2} in 0.95 ± 0.02 N or 4.73 ± 0.11 N NaOH solution in harmony with the reported values.

(4) Observed values of the slope of TAFEL line were satisfactorily explained on the basis of the catalytic mechanism.

From the above mentioned points, it was concluded that the catalytic mechanism is responsible for the hydrogen evolution reaction on Ni in alkaline solutions.

Acknowledgement

The authors wish to express their sincere gratitude to Prof. J. HORIUTI, the director of this Institute, for his many suggestions and useful discussions given throughout this work.

Literature

1) J. HORIUTI and G. OKAMOTO, Sci. Papers Inst. Physics. Chem. Research (Tokyo), **28**, 231 (1936).

2) J. HORIUTI, T. KEII and K. HIROTA, This Journal **2**, 1 (1951-3).

3) A. N. FRUMKIN, V. S. VAGOTZKY, A. Z. JOFA and B. N. KAVANOV, *Kinetics of electrode processes*, Moscow State Univ. Press, 1952. G. KORTÜM, *Lehrbuch der Elektrochemie*, Verlag Chemie G. M. B. H., Weinheim, 1957. J. O'M. BOCKRIS, *Modern Aspects of Electrochemistry*, Butterworth Sci. Pub., 1954.

4) J. HORIUTI, Z. physik. Chem. (N. F.), **15**, 162 (1958).

5) G. OKAMOTO, J. HORIUTI and K. HIROTA, Sic. Papers Inst. Physics. Chem. Research (Tokyo), **29**, 223 (1936).

6) J. HORIUTI, This Journal, **4**, 55 (1956-7).
7) J. HORIUTI, *Trans. Symposium Electrode Processes*, edited by E. YEAGER, p. 17, John Wiley and Sons, Inc., 1961.
8) T. TOYA, This Journal, **6**, 308 (1958), **8**, 209 (1960).
9) J. HORIUTI and T. TOYA, Kinetika i Kataliz, U. S. S. R., **4**, 3 (1963).
10) J. HORIUTI, A. MATUDA, M. ENYO and H. KITA, Reported at the First Australian Conference on Electrochemistry, Sydney/Hobart, 1963. To be published in the Conference Proceedings by Pergamon Press.
11) A. MATUDA and J. HORIUTI, This Journal, **6**, 231 (1958).
12) F. BOWDEN and E. RIDEAL, Proc. Roy. Soc. London, **A120**, 86 (1928). R. JEFFERYS, E. YEAGER and F. HOVORKA, Paper 129. San Francisco Meeting, Electrochemical Society, April 30 to May 3, 1956.
13) P. LUKOVSEV, S. LEVINA and A. FRUMKIN, J. phys. Chem. (U. S. S. R.), **13**, 916 (1936).
14) J. O'M. BOCKRIS and E. C. POTTER, J. Chem. Phys., **20**, 614 (1952).
15) J. O'M. BOCKRIS and A. M. AZZAM, Trans. Faraday Soc., **48**, 145 (1952).
16) B. E. CONWAY, E. M. BEATTY and P. A. DEMAINE, Electrochim. Acta, **7**, 39 (1962).
17) A. C. MAKRIDES, J. Electrochem. Soc., **109**, 977 (1962).
18) A. MATUDA and T. OHMORI, This Journal, **10**, 203 (1962).
19) *idem*, *ibid.*, **10**, 215 (1962).
20) A. M. AZZAM and J. O'M. BOCKRIS, Nature, **165**, 403 (1950).
21) J. HORIUTI, This Journal, **4**, 55 (1956).
22) J. HORIUTI, This Journal, **1**, 8 (1948-51), Bull. Chem. Soc. Japan, **13**, 210 (1938).
23) K. HIROTA and J. HORIUTI, Sci. Papers Inst. Physics. Chem. Research (Tokyo), **34**, 1174 (1938).
24) J. HORIUTI, *Theory of Reaction Rate*, Physical Series X.C.2. Iwanami Book Company, Tokyo, 1940.
25) T. KWAN, This Journal, **1**, 81 (1948-51).
26) T. KWAN, *Advances in Catalysis*, Academic Press Inc., New York, **6**, 67 (1954).
27) A. M. AZZAM, J. O'M. BOCKRIS and H. ROSENBERG, Trans. Faraday Soc., **46**, 918 (1950).
28) For example, E. MATTSON and J. O'M. BOCKRIS, Trans. Faraday Soc., **55**, 1586 (1959).
29) J. O'M. BOCKRIS and H. KITA, J. Electrochem. Soc., **109**, 928 (1962).
30) J. O'M. BOCKRIS, Chem. Rev., **43**, 525 (1948).
31) W. MEHL, M. A. V. DEVANATHAN and J. O'M. BOCKRIS, Rev. Sci. Instr., **29**, 180 (1958).
32) J. CRANK, *The mathematics of Diffusion*, p. 91, Oxford at the Clarendon Press, Oxford (1956).
33) W. M. LATIMER, *Oxidation States of the elements and their Potentials in aqueous solutions*, Prentice-Hall Inc., New York. 1952.
34) LANDOLT und BÖRNSTEIN, *Phys. chem. Tabellen*, Hp IIIa, p. 284.
35) *ibid*, Hp II, p. 1246.
36) *ibid*. Eg IIIc, p. 2373.
37) G. KORTÜM and J. O'M. BOCKRIS, *Text book of electrochemistry*, p. 205, Elsvier Pub. Co., 1951.

38) International Critical Tables, Vol. 5, p. 62.
39) R. CLAMROTH und C. A. KNORR, Z. Elektrochem., **57**, 399 (1953).
40) A. MATUDA, This Journal, **8**, 29 (1960).
41) *idem*, *ibid*, **8**, 151 (1960).
42) J. O'M. BOCKRIS and H. KITA, J. Electrochem. Soc., **108**, 676 (1961).
43) M. ENYO, M. HOSHI and H. KITA, This volume, p. 34.
44) J. HORIUTI, T. KEII, M. ENYO and M. FUKUDA, This Journal, **5**, 40 (1957).
45) E. YEAGER, *Trans. Symposium Electrode Processes*, edited by E. YEAGER, p. 145, John Wiley and Sons. Inc., 1961.